

Multi-layer asymptotic solution for wetting fronts in porous media with exponential moisture diffusivity

By Christopher J. Budd and John M. Stockie

We study the asymptotic behaviour of sharp front solutions arising from the nonlinear diffusion equation $\theta_t = (D(\theta)\theta_x)_x$, where the diffusivity is an exponential function $D(\theta) = D_o \exp(\beta\theta)$. This problem arises in the study of unsaturated flow in porous media where θ represents the liquid saturation. For the physical parameters corresponding to actual porous media, the diffusivity at the residual saturation is $D(0) = D_o \ll 1$ so that the diffusion problem is nearly degenerate. Such problems are characterised by wetting fronts that sharply delineate regions of saturated and unsaturated flow, and that propagate with a well-defined speed. Using matched asymptotic expansions in the limit of large β , we derive an analytical description of the solution that is uniformly valid throughout the wetting front. This is in contrast with most other related analyses that instead truncate the solution at some specific wetting front location, which is then calculated as part of the solution, and beyond that location the solution is undefined. Our asymptotic analysis demonstrates that the solution has a four-layer structure, and by matching through the adjacent layers we obtain an estimate of the wetting front location in terms of the material parameters describing the porous medium. Using numerical simulations of the original nonlinear diffusion equation, we demonstrate that the first few terms in our series solution yields approximations to physical quantities such as wetting front location and speed of propagation that are more accurate (over a wide range of admissible β values) than other asymptotic approximations reported in the literature.

1. Introduction

Problems with exponential diffusivity arise commonly in the study of water transport in variably-saturated porous media such as soil, rock or building materials [4]. An example of such is the one-dimensional nonlinear diffusion problem

$$\frac{\partial \theta}{\partial t} = \frac{\partial}{\partial x} \left(D(\theta) \frac{\partial \theta}{\partial x} \right), \quad (1a)$$

$$\theta(0, t) = \theta_i \quad \text{and} \quad \theta(L, t) = \theta_o \quad \text{for } t \geq 0, \quad (1b)$$

$$\theta(x, 0) = \theta_o \quad \text{for } 0 < x < L, \quad (1c)$$

where the solution $\theta(x, t)$ is called *saturation* and represents the volume fraction of pore space occupied by liquid. We are concerned here with the case when $L \gg 1$ and the diffusivity is an

Address for correspondence: John M. Stockie, Department of Mathematics, Simon Fraser University, 8888 University Drive, Burnaby, BC, V5A 1S6, Canada; email: stockie@math.sfu.ca

exponential function of the solution having the form

$$D(\theta) = D_o e^{\beta\theta}, \quad (1d)$$

where D_o and β are constants satisfying $0 < D_o \ll 1$ and $\beta \gg 1$. Many experimental studies of porous media have been performed in which an exponential diffusion ansatz provides a good fit with measured data, mostly in the context of water transport in soil and rock [4, 5, 11, 17], but also for other porous materials such as wood [20], brick [16] or concrete [10]. Exponential diffusion has also been identified in other transport phenomena as diverse as chemical diffusion kinetics in optical lithography [22] and heat conduction [6].

The significance of this type of diffusion coefficient is that if $\theta_i > \theta_o$ and if β is even moderately large then $D(\theta)$ varies rapidly with θ , thereby causing solutions of (1a) to develop a sharp *wetting front* that is associated with localised high curvature and an exponential change in the solution gradient. The aim of this paper is to perform an asymptotic analysis of this phenomenon and in particular to study self-similar solutions of (1a) using a multi-layer asymptotic expansion, supported by numerical calculations. The asymptotic theory is especially subtle owing to the exponential change in the solution gradient and yields sharp estimates that agree well with numerical simulations.

1.1. Overview of Previous Work

The nonlinear diffusion equation (1a) has been studied in considerable detail for diffusivities $D(\theta)$ having a variety of functional forms. Particular emphasis has been placed on the special case of a power law, $D(\theta) = \theta^m$ with $m > 0$, for which (1a) is called the *porous medium equation* or *PME*; an extensive literature exists for the PME that is thoroughly covered in the review by Vázquez [21]. In a typical wetting scenario the PME is supplemented by boundary conditions $\theta(0, t) = 1$ and $\theta(\infty, t) = 0$, in which case the solution for a power-law diffusivity is well known to have compact support and to consist of a front propagating to the right with speed proportional to $t^{-1/2}$. Ahead of the front, the solution is identically zero and when $m \geq 1$ there is a discontinuity in the first derivative θ_x at the point where the front meets the x -axis; otherwise, when $0 < m < 1$, the wetting front meets the leading edge solution smoothly. The trailing edge of the front on the other hand, always experiences a smooth transition similar to the saturation profile displayed in Figure 2(b). Analytical results have been derived for other forms of the diffusion coefficient, for example by Shampine [18] who provides an existence-uniqueness proof for a general class of diffusivity functions with $D(\theta)$ required to be a continuously differentiable function on $0 \leq \theta \leq 1$, satisfying $D(0) = 0$ and $D(\theta) > 0$ when $\theta > 0$. This and other analytical studies are characterised by the fact that they pertain to *degenerate diffusion* for which the diffusivity vanishes identically at zero saturation.

In contrast with this previous work, the diffusion coefficient we consider in this paper is an exponential function of saturation that, although small, is still bounded away from zero; hence the solution remains everywhere classical and all disturbances propagate with infinite speed, analogous to solutions of the “usual” heat equation. When the PME wetting scenario described above is repeated for an exponential diffusivity, the solution remains non-zero for all times $t > 0$, even when the initial conditions have bounded support. Nonetheless, this problem can be *nearly degenerate* in the sense that $D(0) \ll 1$ whereas $D(\theta) = \mathcal{O}(1)$ for θ away from zero. For example, typical parameter values for porous soils have been estimated as $D_o \approx 2 \times 10^{-9} \text{ m}^2/\text{s}$ and $\beta \approx 20$ [17]. For such diffusion coefficients, the solution inherits features that are qualitatively similar to the degenerate problem, most notably a steep wetting front that propagates with finite speed and that is associated with localised high curvature (see Figure 1(b)). We define the wetting front location $x_*(t)$ to be the point where the curvature in $\theta(x, t)$ is greatest, and for $x > x_*$ we have that $\theta_x \ll 1$. One feature that distinguishes the exponential diffusion equation from the PME is the fact that θ

exhibits more rapid variations than for a power law, which in turn has a substantial impact on the shape of the solution close to the wetting front. A direct comparison is afforded by Leech et al.'s study of concrete [10] wherein they use experimental data to fit both power-law and exponential diffusivities, yielding respectively $D(\theta) = D_o\theta^4$ and $D(\theta) = D_o e^{6(\theta-1)}$. In Figure 1, we plot the diffusion coefficients and corresponding saturation profiles for these two choices of $D(\theta)$. While the qualitative features of both solutions are similar, there is a significant difference in both the steepness and location of the wetting front, as well as the sharpness of the corner (refer to the zoomed-in region in Figure 1(b)). Another distinguishing feature is that the solution in the exponential case is characterized by a small nonzero saturation ahead of the wetting front.

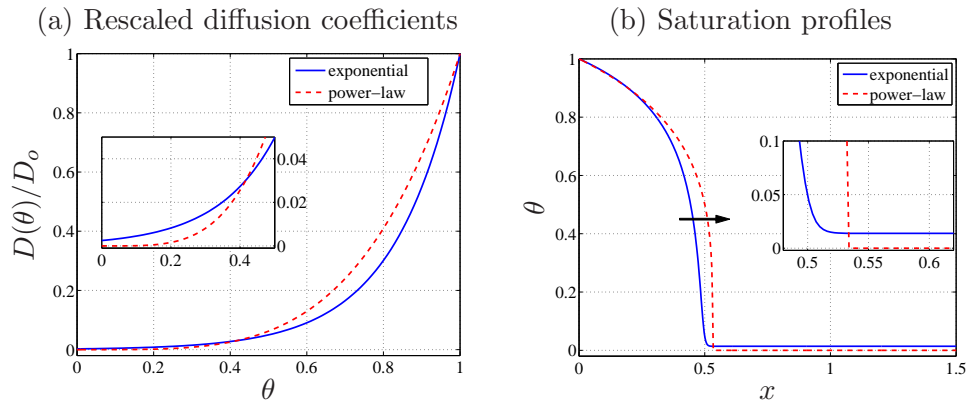


Figure 1. Comparison of solutions to the nonlinear diffusion problem for power-law and exponential diffusion coefficients, $D(\theta) = D_o\theta^4$ and $D(\theta) = D_o e^{6(\theta-1)}$. (a) On the left is the rescaled diffusivity $D(\theta)/D_o$. (b) On the right are the corresponding saturation profiles $\theta(x, t)$ computed numerically at some fixed time $t > 0$. The horizontal arrow indicates the direction of the wetting front motion (from left to right).

Following up on these experimental studies, several authors have derived theoretical results for the exponential diffusion problem. Crank's book [7] provides a comprehensive treatment of analytical solutions for nonlinear diffusion equations circa 1975 with many forms of the diffusivity function. In particular, Crank derives a similarity solution for the exponential diffusion case (following the work of Cooper [6]) that reduces the problem to a second-order ordinary differential equation (ODE) which he then solves numerically – indeed, this is the same ODE that we will present later in Section 3. An alternate approach using functional iteration has been developed based on an integral formulation of the governing equations by Parslow et al. [15].

In contrast with these iterative or numerical solution methods, we are interested here in developing an asymptotic series representation of the solution. One study of particular relevance is due to Babu [2] who derived an asymptotic solution by making use of the simplifying assumption that both saturation and diffusivity drop to zero ahead of a certain wetting front location. Although Babu's asymptotic estimates are reasonably accurate, we will demonstrate that his approach of truncating the solution at the wetting front introduces significant errors that can be reduced by considering an alternate approach that incorporates the effect of the extremely small but still nonzero diffusivity values ahead of the front. Other alternate series expansions based on an integral form of the exponential diffusion equation were derived by Parlange and co-workers in [13, 14]. Finally, we point out a connection to the work of Elliott et al. [8] who applied methods from singular perturbation theory to analyse the detailed structure of the transition region for the power-law diffusivity in

the limiting case of $m \rightarrow \infty$, which is known as the *mesa problem*. Although this problem is still degenerate, the diffusivity in the large- m limit experiences a rate of increase in θ approaching that of an exponential function; therefore, the analysis for the mesa problem can be considered as a prototype for problems such as (1).

1.2. Summary of Main Results

We will demonstrate in this paper that a multi-layer asymptotic expansion is capable of yielding an accurate estimate of the wetting front location, provided that the exponentially varying solution is properly resolved close to the front. In particular, we will show that there is a self-similar solution with a wetting front at position

$$x_*(t) = y_* \sqrt{2tD(\theta_i)}.$$

The constant y_* is the location of the front in terms of a similarity variable $\Theta(y)$ and has the asymptotic expansion

$$y_* = \frac{1}{\gamma} + \frac{1}{2\gamma^3} + \frac{11}{12\gamma^5} + \mathcal{O}\left(\frac{1}{\gamma^7}\right).$$

The large parameter $\gamma = -\Theta'(0)$ represents the initial slope of the similarity solution, and is related to the physical constant β through the asymptotic expression

$$\bar{\beta} \equiv \beta(\theta_i - \theta_o) = \gamma^2 + \frac{1}{2} + \frac{\alpha_3}{\gamma^2} + \mathcal{O}\left(\frac{1}{\gamma^4}\right) \gg 1,$$

where $\alpha_3 \approx \frac{1}{12}$ is obtained numerically. Our asymptotic solution is distinct from other approximations derived in the literature in that it provides insight into the detailed structure of the wetting front, as well as yielding estimates of quantities such as the wetting front location that are accurate over a wide range of physical parameters.

The remainder of this paper is structured as follows. In Section 2 we motivate the problem under study by using the example of water transport in unsaturated porous media. In Section 3 we introduce a similarity transformation that permits us to recast problem as an ODE initial value problem, for which $\gamma \gg 1$ corresponds to the magnitude of the initial slope of the similarity solution. Section 4 derives our key results, consisting of a four-layer asymptotic expansion for the similarity solution, expressed as a series in γ on each layer. Matching the asymptotic expressions then yields series approximations for the quantities of physical interest such as the saturation and curvature at the sharp corner in the wetting front, as well as the location x_* of the front itself. In Section 6 we perform a detailed comparison of our asymptotic solution to other approximations in the literature, as well as validating the results with careful numerical simulations of the original governing partial differential equation.

2. Physical Background

Water transport in a saturated porous medium is well-known to obey Darcy's law [3], $\mathbf{U} = -K\nabla\Phi$, which states simply that the liquid velocity \mathbf{U} (in m/s) is proportional to the gradient of total hydraulic potential Φ (in m). The proportionality constant K is known as the hydraulic conductivity and has units of m/s . However, many porous media flows are unsaturated, which means that the pore volume is only partially filled with liquid, and in this case it is necessary to introduce the liquid volume fraction or saturation, θ . The conductivity in a variably saturated porous

medium is typically assumed to depend on the local saturation, leading to an extended Darcy’s law, $\mathbf{U} = -K(\theta) \nabla \Phi$, that includes a saturation-dependence in the hydraulic conductivity. When this expression for velocity is substituted into the continuity equation

$$\frac{\partial \theta}{\partial t} + \nabla \cdot \mathbf{U} = 0,$$

we obtain an evolution equation for θ

$$\frac{\partial \theta}{\partial t} = \nabla \cdot (K(\theta) \nabla \Phi), \tag{2}$$

which is known as the *Richards equation*. If both Φ and K are assumed to be single-valued functions of saturation, then we can define $D(\theta) := K(\theta) (d\Phi/d\theta)$ after which Eq. (2) reduces to the familiar nonlinear diffusion equation

$$\frac{\partial \theta}{\partial t} = \nabla \cdot (D(\theta) \nabla \theta),$$

for which Eq. (1a) is the 1D version. The function $D(\theta)$ is referred to as the *moisture diffusivity* and has units of m^2/s . As mentioned in the Introduction, the exponential form (1d) for diffusivity is motivated by the study of certain soils and porous building materials, for which an exponential function provides a good fit to experimental data.

We consider an idealised, cylindrical geometry depicted in Figure 2 that is consistent with the samples typically used in experimental studies of moisture transport. The porous cylinder is initially

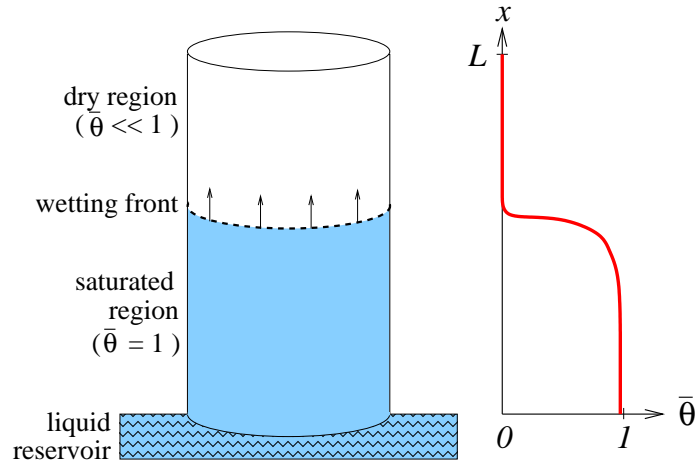


Figure 2. Left: A cylindrical porous medium with one end immersed in a water reservoir, depicting the upward progress of a wetting front owing to capillary action. Right: Rescaled saturation $\bar{\theta}$ along the length of the cylinder from $x = 0$ to L .

dry and has one end placed in a water reservoir. For the problems of interest here, capillary forces dominate over gravity and so we can assume that water is absorbed into the porous medium by capillary action alone. Water progresses into the sample in the form of a nearly planar wetting front that propagates vertically upwards. We assume therefore that the flow is uni-directional and governed by the one-dimensional diffusion equation (1a). The length of the sample is denoted by L , which is presumed large in relation to the diameter so that $L \gg 1$.

In order to treat a general class of wetting scenarios we take samples that are never completely dry, which corresponds to the usual situation wherein a porous medium undergoes re-wetting after an initial wetting/drainage cycle. Consequently, there exists a non-zero minimum or residual saturation $\theta = \theta_o$ deriving from water that is trapped in isolated portions of the porous matrix and which cannot be displaced by capillary action. Furthermore, we introduce a maximum saturation $\theta_i \leq 1$ that cannot be exceeded owing to micropores that are too small to allow water to penetrate, no matter how large the capillary force. Consequently, the saturation θ satisfies $0 < \theta_o \leq \theta \leq \theta_i \leq 1$, while the boundary and initial conditions are as specified in (1b) and (1c). Water content is usually reported in the literature in terms of *reduced saturation*

$$\bar{\theta} = \frac{\theta - \theta_o}{\theta_i - \theta_o} = \frac{\theta - \theta_o}{\Delta\theta},$$

for which the boundary and initial conditions reduce to

$$\bar{\theta}(0, t) = 1, \quad \bar{\theta}(L, t) = 0 \quad \text{and} \quad \bar{\theta}(x, 0) = 1. \quad (3)$$

A picture of a typical wetting front is displayed in Figure 2 (right) in terms of the rescaled saturation variable $\bar{\theta}$.

3. Self-Similar Solution

We are now interested in finding a self-similar solution of the nonlinear diffusion equation on the half-space $x \in [0, \infty]$. The problem (1) is invariant under the scaling transformation

$$y = x/t^\xi, \quad (4)$$

which motivates us to seek a general solution of the form

$$\theta(x, t) = \Psi(y) + \zeta \log(t), \quad (5)$$

where ξ and ζ are constants. Upon substituting these expressions into Eqs. (1a) and (1d) we obtain

$$\zeta - \xi y \Psi' = D_o t^{\beta\zeta - 2\xi + 1} \left(e^{\beta\Psi} \Psi' \right)',$$

which is a true self-similar solution if the parameters satisfy $\beta\zeta - 2\xi + 1 = 0$. After imposing the first boundary condition (1b), Eqs. (4)–(5) require that $\zeta = 0$ and $\xi = \frac{1}{2}$, leading to the self-similar solution $\theta(x, t) = \Psi(y)$ with $y \propto x/t^{1/2}$. This form of solution is consistent with the second boundary condition in (1b) provided that $L \gg t^{1/2}$, which motivates our taking $L \rightarrow \infty$ in what follows. It is convenient to take the following scaled form of the similarity variable

$$y = \frac{x}{\sqrt{2tD(\theta_i)}}, \quad (6)$$

which is chosen to eliminate certain constants from the ODE and boundary conditions. We then define a new dependent variable

$$\Theta(y) = e^{\beta(\theta - \theta_i)} \quad \text{or equivalently} \quad \Theta(y) = e^{\bar{\beta}(\bar{\theta} - 1)}, \quad (7)$$

where $\bar{\beta} := \beta\Delta\theta = \beta(\theta_i - \theta_o)$. This simplifies the problem further by eliminating the exponential diffusion coefficient (1d), leading to the following ODE boundary value problem for $\Theta(y)$:

$$\Theta\Theta'' = -y\Theta' \quad \text{for } 0 < y < \infty, \quad (8a)$$

$$\Theta(0) = 1, \quad (8b)$$

$$\Theta(\infty) = \Theta_\infty := e^{-\bar{\beta}}. \quad (8c)$$

For the porous media of interest here, $\bar{\beta}$ is significantly greater than one so that the parameter Θ_∞ satisfies $0 < \Theta_\infty \ll 1$.

Rather than solving Eqs. (8) directly it is convenient to reformulate this boundary value problem as an initial value problem, in which the boundary condition (8c) is replaced by a second initial condition

$$\Theta'(0) = -\gamma, \quad (8c')$$

where $\gamma > 0$ represents the magnitude of the initial slope. From this point on, we use (8') to refer to the initial value problem consisting of equations (8a), (8b) and (8c'). The asymptotic analysis performed in this paper considers the limit of $\gamma \rightarrow \infty$ which we will see shortly is equivalent to taking $\Theta_\infty \rightarrow 0$. The quantity γ is not known *a priori* in terms of the physical parameters, and so one of the primary results of this paper will be to derive asymptotic expressions for $\bar{\beta}$ and y_* in terms of γ .

3.1. Preliminary Numerical Simulations

Before proceeding with the analysis, we present several plots that illustrate the asymptotic behaviour of the self-similar solution for large γ , computed via numerical simulations of the initial value problem (8'). We use a shooting algorithm wherein a value of $\bar{\beta}$ is chosen, and then the initial slope $\gamma = -\Theta'(0)$ is updated iteratively until Θ is sufficiently close to the right hand boundary value $\Theta_\infty = e^{-\bar{\beta}}$. This approach is similar to that employed by others for the exponential diffusion problem [7, 23], and more details on our shooting algorithm are given in Section 6.1. For illustration purposes, we choose physical parameters corresponding to a typical soil water uptake experiment [17]. Taking limiting values of $\theta_o = 0.04$ and $\theta_i = 0.43$ and an unsaturated diffusivity $\beta = 20.5$, we obtain parameters $\Delta\theta = 0.39$, $\Theta_\infty = 3.4 \times 10^{-4}$ and $\bar{\beta} = 8$ for which $D(0) = \exp(-8) \ll 1$. We remark that other experiments on water transport in a wide range of porous media (including soils, concrete, and other building materials) suggest that allowable values of $\bar{\beta}$ are restricted to a fairly narrow interval of $4 \lesssim \bar{\beta} \lesssim 9$. The resulting numerical solution is depicted in the two rightmost plots in Figure 3(c). The upper plot displays the computed similarity solution $\Theta(y)$ while the lower plot shows the corresponding curves for reduced saturation $\bar{\theta}(x, t)$ at ten equally-spaced time intervals, which are determined from $\Theta(y)$ by transforming back to physical variables Eq. (6).

The computed solution for $\bar{\beta} = 8$ exhibits a well-defined wetting front that is manifested in the $\bar{\theta}$ plot as a narrow region with a steep slope located immediately behind a sharp corner. In the plot of Θ on the other hand, the step front has been eliminated by the exponential stretching transformation (7), but the wetting front location is still identified with a sharp corner. A zoomed-in view of the wetting front is shown in the inset for $\bar{\beta} = 8$ and clearly indicates that the solution within the corner region transitions rapidly to a small value of saturation, but this transition nonetheless remains smooth.

Additional pairs of solution plots are provided in Figures 3(a,left) and 3(b,middle) for values of $\bar{\beta} = 2$ and 4 respectively. Clearly, taking $\bar{\beta}$ smaller (or equivalently Θ_∞ larger) causes the wetting front to exhibit a more gradual slope and a milder transition through the corner region, and in

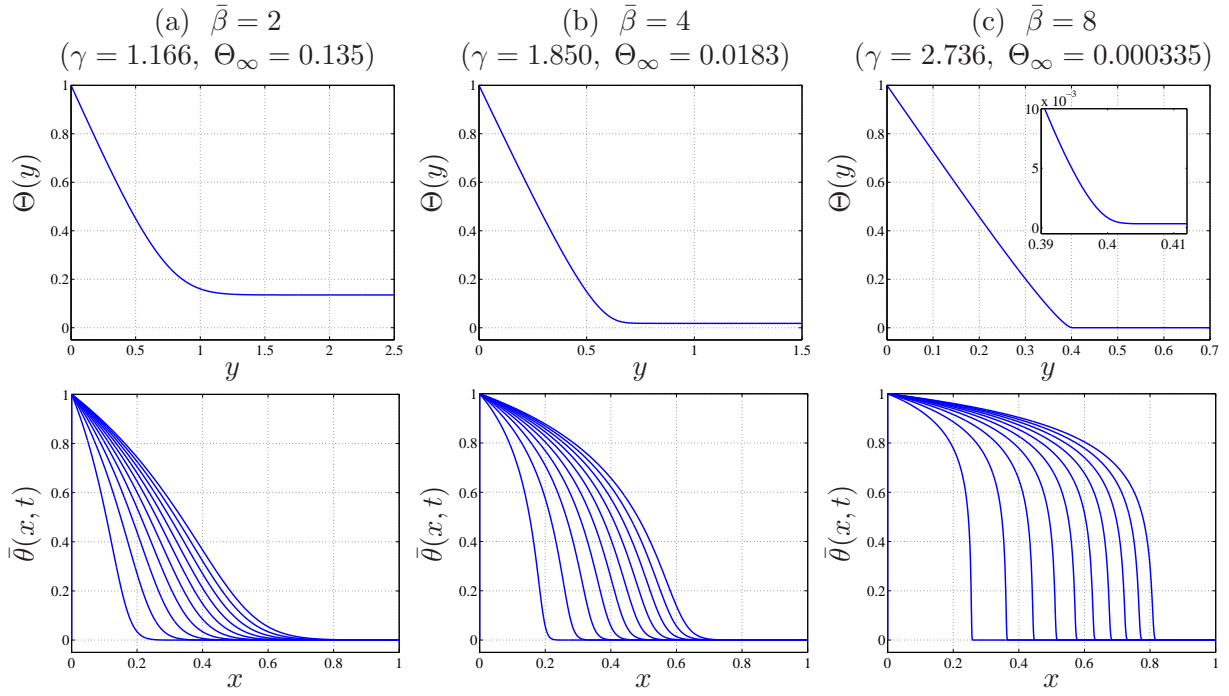


Figure 3. Saturation for values of $\bar{\beta} = \beta\Delta\theta = 2$ (left), 4 (middle) and 8 (right). The top row shows the similarity variable $\Theta(y)$ obtained by solving Eqs. (8') numerically. The bottom row contains corresponding plots of the reduced saturation, $\bar{\theta}(x, t) = 1 + (\log \Theta)/\bar{\beta}$, with time t taken at ten equally-spaced points. The inset at the top right is a zoomed-in view of the sharp corner.

the extreme case of $\bar{\beta} = 2$ there is hardly any evidence of a wetting front at all. However, as we have indicated above, most problems of physical interest correspond to values of $\bar{\beta} \geq 4$ and this observation has an important effect on the accuracy of our asymptotic solution derived in Section 4.

We next investigate in more detail the effect on the similarity solution $\Theta(y)$ of changes in $\bar{\beta}$. In particular, Figure 3 indicates that the initial slope γ increases as $\bar{\beta}$ increases, with a corresponding shift of the wetting front location closer to the origin along the y -axis. A number of additional simulations are performed for γ lying in the interval $[0.5, 5.0]$ and the corresponding values of $\bar{\beta}$ are plotted in Figure 4(a). By performing a least-squares polynomial fit to the computed points, we obtain to a very good approximation the following quadratic polynomial fit

$$\bar{\beta} = -\log \Theta_\infty \approx \gamma^2 + \frac{1}{2},$$

which when displayed in Figure 4(a) alongside the computed data is nearly indistinguishable. This relationship between $\bar{\beta}$ and γ will be verified later in Section 4 when it is derived as part of our asymptotic solution.

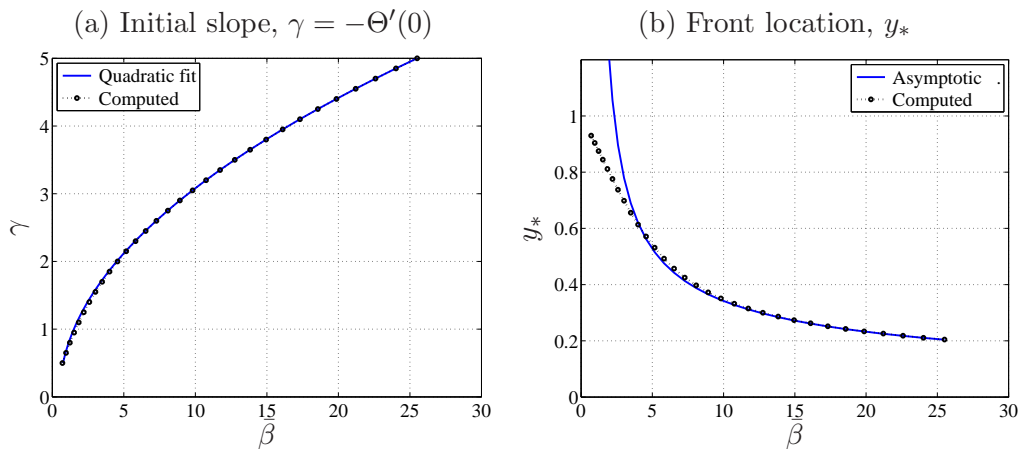


Figure 4. Left: Values of $\bar{\beta}$ and $\gamma = -\Theta'(0)$ obtained from numerical simulations of Eq. (8') with parameters chosen as in Figure 3. The quadratic fit $\bar{\beta} = \gamma^2 + 1/2$ is shown as a solid line for comparison purposes. Right: The computed wetting front location (estimated using the point of maximum curvature) is depicted along with the two-term asymptotic approximation from Eq. (20).

It is evident from the plots in Figure 3 that for $\bar{\beta}$ sufficiently large there exists a sharp corner in the similarity solution $\Theta(y)$ that can be identified with the wetting front location in plots of saturation $\bar{\theta}$. In contrast with the power-law diffusion problem, where the wetting front is identified with a discontinuity in the solution derivative, the exponential diffusion problem exhibits a smooth transition through the front and so there is no unique front position. We therefore choose to identify the wetting front location y_* with the point of maximum curvature in Θ which satisfies $\Theta''(y_*) = 0$. We provide a preview of our asymptotic results in Figure 4(b), which depicts the computed front location y_* as a function of $\bar{\beta}$, alongside our two-term asymptotic approximation of y_* derived later in Section 4.2. Clearly, the analytical results are quite accurate for $\bar{\beta}$ in the physical range.

4. Multi-Layer Asymptotic Solution

In this section, we will derive the asymptotic form of the solution for large γ . The preliminary numerical results already shown in Figure 3 suggest that the solution for large $\bar{\beta}$ (and hence large γ) should be separated into four regions or layers:

- A nearly linear *inner solution* that extends over a range of y values lying between 0 and slightly below y_* .
- A nearly constant *outer solution* on the right of y_* that approaches Θ_∞ for y sufficiently large.
- A *mid-range solution* that provides a smooth transition between the inner and outer solutions for intermediate values of y close enough to y_* . Because of the exponential variation of the solution through the corner of the wetting front, it will prove necessary to divide the mid-range into a *left mid-range* and *right mid-range solution*.

These four regions are depicted schematically in Figure 5 in terms of the similarity variable $\Theta(y)$. We note that a rough approximation of the wetting front location is given by $y_* \approx 1/\gamma$, determined as the y -intercept of the straight line having the same initial slope $\Theta'(0)$; in fact, this is the leading order term in the asymptotic expansion we derive later in this section. We expect that this approximation will be inaccurate for small values of $\bar{\beta}$ when the inner solution is more curved behind the front location, but will improve as $\bar{\beta}$ increases and the inner solution is closer to linear.

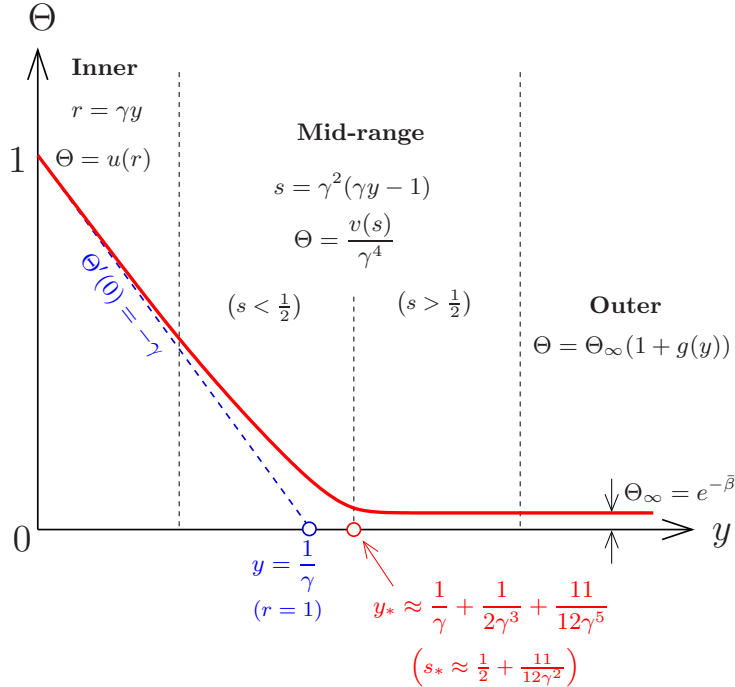


Figure 5. The similarity solution $\Theta(y)$ is separated into several regions: an inner region on the left consisting of a nearly linear solution $u(r)$; an outer region on the right which is nearly constant; and an intermediate region near the wetting front location $y = y_*$ within which a mid-range solution connects the inner and outer solutions. It is necessary to subdivide the mid-range solution further into two pieces, to the left and the right of y_* .

With the preceding discussion in mind we now look for a four-layer asymptotic series solution to Eq. (8'), where the solution in each layer is expressed in terms of an appropriately scaled independent variable and expanded as a series in $1/\gamma$ for large γ . The four solutions will then be matched in order to derive a series solution that is valid over the entire range of y . In practice, we will see that γ need not be very large at all for the asymptotic solution to be a reasonable approximation; in fact, the series will converge so rapidly that taking $\gamma > 1$ is usually sufficient! In the following sections, we derive the leading order terms in the asymptotic expansion for each of the inner, outer and mid-range solutions. Then by matching the corresponding solutions at the interior layer boundaries, we will obtain an approximation of the front location y_* in terms of γ which will then permit us to estimate γ , and hence also y_* , in terms of the known physical parameters.

Before going into the details, we first summarise the main result for the wetting front location

$$y_* = \frac{1}{\gamma} + \frac{1}{2\gamma^3} + \frac{11}{12\gamma^5} + \mathcal{O}\left(\frac{1}{\gamma^7}\right). \quad (9)$$

By taking y_* to be the point of maximum curvature in saturation $\Theta(y)$, we may then approximate the values of both saturation and curvature at the wetting front by

$$\Theta(y_*) \approx e\Theta_\infty \quad \text{and} \quad \Theta''(y_*) \approx \frac{1}{\gamma^2}e^{\gamma^2-1/2}. \quad (10)$$

We will show further that

$$\Theta\left(\frac{1}{\gamma}\right) = \frac{1}{2\gamma^2} + \frac{\alpha_2 - \log(\gamma)}{\gamma^4} + \mathcal{O}\left(\frac{1}{\gamma^6}\right) \quad \text{where} \quad \alpha_2 = \frac{11}{12} - \frac{1}{2}\log 2. \quad (11)$$

Finally, the physical parameter $\bar{\beta}$ can be expressed as

$$\bar{\beta} = -\log \Theta_\infty = \gamma^2 + \frac{1}{2} + \frac{\alpha_3}{\gamma^2} + \mathcal{O}\left(\frac{1}{\gamma^4}\right) \quad (12)$$

where α_3 is a constant that we estimate numerically to be $\alpha_3 = 1/12$. It follows immediately that for large $\bar{\beta}$ we have

$$\gamma = \bar{\beta}^{1/2} - \frac{1}{4}\bar{\beta}^{-1/2} - \left(\frac{\alpha_3}{2} - \frac{1}{32}\right)\bar{\beta}^{-3/2} + \mathcal{O}\left(\bar{\beta}^{-5/2}\right). \quad (13)$$

4.1. Preliminary Estimate of the Leading Order Asymptotic Form

Before getting into the details of the derivation we begin with a simple calculation that aims to establish, without any attempt at rigour, the leading order asymptotic form of the solution to equations (8'), which we repeat below for convenience:

$$\Theta\Theta'' = -y\Theta', \quad \Theta(0) = 1, \quad \Theta'(0) = -\gamma, \quad \Theta(\infty) = \Theta_\infty.$$

We remark that standard methods of analysis show that $\Theta > 0$ and $\Theta' < 0$ for all y , so that $\Theta \rightarrow \Theta_\infty$ and $\Theta' \rightarrow 0$ as $y \rightarrow \infty$. Now, if we divide both sides of the ODE by y , then integrate and apply boundary conditions, we obtain

$$-\log(\Theta_\infty) = \int_0^\infty \frac{\Theta''(y)}{y} dy. \quad (14)$$

In the case when γ is large, our previous numerical calculations show that:

- (a) $\Theta' \approx -\gamma$ if $0 \leq y < 1/\gamma$;
- (b) $\Theta' \approx 0$ if $y > 1/\gamma$;

- (c) $\Theta'' \approx 0$ if $y \neq 1/\gamma$; and
- (d) $\Theta''(1/\gamma) \gg 1$.

It follows from these observations that

$$\int_0^\infty \frac{\Theta''}{y} dy \approx \gamma [\Theta']_{1/\gamma^-}^{1/\gamma^+} \approx \gamma^2,$$

which can be combined with (14) to obtain the leading order estimate

$$-\log \Theta_\infty \approx \gamma^2. \quad (15)$$

While this estimate is not precise, we can use this simple calculation as a guide in the subsequent development of the asymptotic theory.

4.2. Inner Solution

On the interval $0 \leq y \lesssim y_*$, we know that the solution slope is initially $-\gamma$ and so it is natural to introduce a new independent variable $r = \gamma y$ and define the inner solution as $u(r) = \Theta(y)$. Rescaling Eqs. (8') yields

$$u u'' = -\frac{r u'}{\gamma^2}, \quad (16a)$$

$$u(0) = 1, \quad (16b)$$

$$u'(0) = -1. \quad (16c)$$

The $1/\gamma^2$ factor on the right hand side of (16a) suggests using for an asymptotic expansion of the form

$$u(r) = u_0(r) + \frac{u_1(r)}{\gamma^2} + \frac{u_2(r)}{\gamma^4} + \mathcal{O}\left(\frac{1}{\gamma^6}\right). \quad (17a)$$

After substituting this expression into the ODE and boundary conditions for u , we obtain the following sequence of initial value problems up to $\mathcal{O}(\gamma^{-4})$:

$$\begin{aligned} u_0 u_0'' &= 0, & u_0(0) &= 1, & u_0'(0) &= -1, \\ u_0 u_1'' &= -r u_0', & u_1(0) &= 0, & u_1'(0) &= 0, \\ u_0 u_2'' &= -u_1 u_1'' - r u_1', & u_2(0) &= 0, & u_2'(0) &= 0. \end{aligned}$$

These problems can be integrated successively to obtain

$$u_0 = 1 - r, \quad (17b)$$

$$u_1 = \frac{1}{2} - \frac{1}{2}(1-r)^2 + (1-r) \log(1-r), \quad (17c)$$

$$u_2 = \frac{17}{12} - \frac{3}{4}(1-r) - \frac{3}{4}(1-r)^2 + \frac{1}{12}(1-r)^3 + \left(2 - \frac{3}{2}r\right) \log(1-r), \quad (17d)$$

which after substitution into (17a) gives the inner solution to $\mathcal{O}(\gamma^{-4})$. The $\mathcal{O}(1)$ and $\mathcal{O}(\gamma^{-2})$ solutions are depicted in Figure 6 for values of $\beta = 2, 4$ and 8 . Plots of the numerical solution of Eqs. (8'), computed using the shooting algorithm described in Section 6 (and labeled ‘‘Exact’’) have also been included for comparison purposes. From these plots, the logarithmic breakdown in u_1 as $r \rightarrow 1^-$ is apparent. We note also that including the u_2 term makes no difference to the naked eye, but this term is necessary in order to complete the asymptotic matching procedure later on in Section 4.3.1.

We now investigate more carefully the validity of these asymptotic expressions. It is immediately clear that the terms u_1 and u_2 contain a logarithmic singularity as $r \rightarrow 1$ (i.e., $y \rightarrow 1/\gamma$) and hence the inner solution cannot be valid up to and including $r = 1$; in fact, our expansion (17a) is valid when

$$\gamma^2(1-r) \gg 1 \quad \text{or alternately} \quad y \ll \frac{1}{\gamma} - \frac{1}{\gamma^3}. \quad (18)$$

To see this more clearly, we require for asymptotic regularity that

$$u_0(r) \gg \frac{u_1(r)}{\gamma^2}.$$

Taking the leading order term on each side of this equation yields

$$(1-r) \gg \frac{1}{2\gamma^2},$$

which upon rescaling identifies the *inner range* over which the inner solution is valid to be

$$0 \leq y < \frac{1}{\gamma} - \mathcal{O}\left(\frac{1}{\gamma^3}\right). \quad (19)$$

Finally, we discuss how the first two terms in the asymptotic expansion (17) may be used to estimate the wetting front location y_* by considering the limit as $r \rightarrow 1^-$, but not so close to 1 that the logarithmic singularity takes effect. To this end, we set $u_0 + u_1/\gamma^2 = 0$ and neglect terms that are quadratic and logarithmic in $(1-r)$ to obtain

$$y_* \approx \frac{1}{\gamma} + \frac{1}{2\gamma^3}, \quad (20)$$

which yields the first two terms in the front location (9). Notice that the leading order approximation $y_* \approx 1/\gamma$ corresponds to the intersection point where the linear solution u_0 meets the y -axis. One of the primary aims of the asymptotic matching performed in Section 4.4 is to derive a correction to Eq. (20) that gives a more refined estimate of y_* .

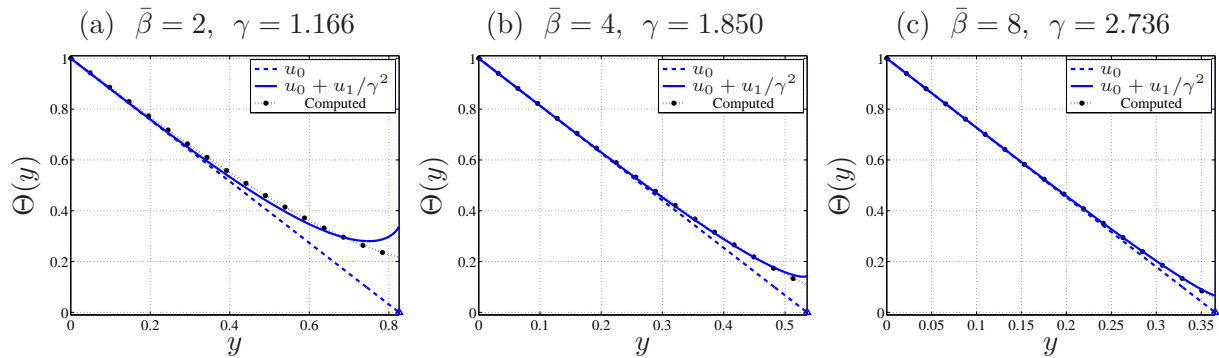


Figure 6. The inner solution $u(r)$ for values of $\bar{\beta} = 2, 4$ and 8 , showing the leading order approximation u_0 , first order correction $u_0 + u_1/\gamma^2$, and numerical solution of the ODE initial value problem. The point where the approximation u_0 touches the y -axis (Δ) corresponds to the leading order estimate of the wetting front location, $y_* \approx 1/\gamma$.

4.3. Mid-Range Solution

The mid-range encompasses the wetting front near $y \approx y_*$ and is the region where the similarity solution changes rapidly. Accordingly, the mid-range also poses the most subtle challenges for our asymptotic calculation. Within the mid-range, we first determine an appropriate rescaling of the spatial variable y and dependent variable Θ by studying the form of the inner solution as y approaches $1/\gamma$ from the left, or $r \rightarrow 1^-$. In this limit, the dominant terms in the inner expansion (17) are

$$u(r) = 1 - r + \frac{1}{\gamma^2} \left(\frac{1}{2} + \dots \right), \quad (21)$$

(before the logarithmic term takes effect) which agrees with the results depicted in Figure 6. In the mid-range, we seek a solution for which $\Theta \ll 1$ and the first few terms in $u(r)$ balance, thereby requiring that $r = \gamma y = 1 + \mathcal{O}(\gamma^{-2})$. Consequently, we make use of the transformation

$$y = \frac{1}{\gamma} + \frac{s}{\gamma^3} = \frac{1}{\gamma} \left(1 + \frac{s}{\gamma^2} \right), \quad (22)$$

using the new independent variable s which is $\mathcal{O}(1)$, and the mid-range asymptotic series is valid when

$$1 \ll |s| \ll \gamma^2.$$

Observe that the estimate for the wetting front location from Eq. (20) is recovered by simply taking $s = 1/2$ in Eq. (22). The mid-range therefore overlaps with the inner region when $s < 1/2$ and $|s| \gg 1$. In fact, we need to consider two separate mid-range expansions for $s < 1/2$ and $s > 1/2$, and then match each to the inner and outer solution respectively. The overlap region in both cases corresponds to values of $|s| = \mathcal{O}(\gamma)$ for large γ .

The corresponding mid-range scaling for the similarity solution $\Theta(y)$ is found by substituting Eq. (22) into the ODE (8a), which becomes $\Theta \Theta_{ss} = -\Theta_s/\gamma^4$. We are then led to define a new mid-range saturation variable $v(s) = \gamma^4 \Theta(y)$ that obeys

$$v v'' = - \left(1 + \frac{s}{\gamma^2} \right) v'. \quad (23)$$

As $s \rightarrow \infty$ the mid-range solution should match with the outer solution so that

$$v(s) \rightarrow v_\infty := \gamma^4 \Theta_\infty \quad \text{as } s \rightarrow \infty. \quad (24)$$

Integrate Eq. (23) over the interval $[s, \infty)$ to obtain

$$\log(v(s)) - \log(v_\infty) = \int_s^\infty \frac{v'' ds}{(1 + s/\gamma^2)}.$$

The denominator in the integrand can be expanded as a geometric series when $|s| < \gamma^2$ so that

$$\log(v(s)) - \log(v_\infty) = \int_s^\infty v'' \left(1 - \frac{s}{\gamma^2} + \mathcal{O}\left(\frac{s^2}{\gamma^4}\right) \right) ds.$$

Using integration by parts and applying the far field condition $v' \rightarrow 0$ for large s , we find that

$$\log(v) - \log(v_\infty) = -v' \left(1 - \frac{s}{\gamma^2} \right) + \frac{(v - v_\infty)}{\gamma^2} + \mathcal{O}\left(\frac{1}{\gamma^4}\right),$$

which can be rearranged to obtain

$$v' = \log(v_\infty) - \log(v) + \frac{sv'}{\gamma^2} + \frac{1}{\gamma^2}(v_\infty - v) + \mathcal{O}\left(\frac{1}{\gamma^4}\right). \quad (25)$$

Based on this last equation, we can make two observations:

- (i) The derivative v' is strictly negative since $s < \gamma^2$ and $v > v_\infty$ in the mid-range.
- (ii) The only point where $v' \approx 0$ is $v = v_\infty$.

Consequently, the mid-range solution $v(s)$ must be a monotonically decreasing function that asymptotes toward the value v_∞ for large s , which is consistent with the numerical results plotted earlier in Figure 3.

In the next two sections, we develop two asymptotic expansions for the solution of Eq. (25): one valid for $s < 1/2$ (allowing for large negative values of s) and a second valid for $s > 1/2$ (corresponding to large positive values of s).

4.3.1. Mid-range Solution for $s < 1/2$, and Matching to the Inner Solution. The scaling of the mid-range solution for $s < 1/2$ is peculiar, and so we will write the solution in a particular form that simplifies the matching, and justify this choice later on. We take

$$v(s) = \gamma^2 v_0(s) + v_1(s) + \mathcal{O}\left(\frac{1}{\gamma^2}\right) \quad \text{when } s < \frac{1}{2}, \quad (26)$$

and assume that $v_1(s)$ has terms of both $\mathcal{O}(1)$ and $\mathcal{O}(\log \gamma)$. We assume further that

$$v(0) = \frac{\gamma^2}{2} + a \log \gamma + b + \mathcal{O}\left(\frac{1}{\gamma^2}\right), \quad (27)$$

$$\log v_\infty = -\gamma^2 + c \log \gamma + d + \mathcal{O}\left(\frac{1}{\gamma^2}\right), \quad (28)$$

which will be used to find the functions $v_0(s)$ and $v_1(s)$ as well as values of the constants a , b , c , d . We next substitute the expressions (26)–(28) into (25) and solve the equations arising at each order. Considering first the leading terms of $\mathcal{O}(\gamma^2)$, we find that

$$v_0' = -1, \quad v_0(0) = \frac{1}{2},$$

which has solution

$$v_0(s) = \frac{1}{2} - s. \quad (29)$$

Next, take the terms of $\mathcal{O}(1, \log \gamma)$ for which we first need to expand $\log v$ from Eq. (25) as a series in γ

$$\log v = \log\left(\gamma^2\left(\frac{1}{2} - s\right) + v_1 + \dots\right) = 2 \log \gamma + \log\left(\frac{1}{2} - s\right) + \mathcal{O}\left(\frac{1}{\gamma^2}\right),$$

where we have used the fact that $v_0 > 0$ when $s < 1/2$. The $\mathcal{O}(1, \log \gamma)$ equations then reduce to

$$v_1' = (c - 2) \log \gamma + \left(d - \frac{1}{2}\right) - \log\left(\frac{1}{2} - s\right),$$

which can be integrated to obtain

$$v_1(s) = (c-2)s \log \gamma + \left(d - \frac{1}{2}\right)s + a \log \gamma + b + \left(\frac{1}{2} - s\right) \log \left(\frac{1}{2} - s\right) + s - \frac{1}{2} \log 2. \quad (30)$$

We now proceed to match the mid-range expansion $v = \gamma^2 v_0 + v_1$ to the inner solution in the limit where both $-s, \gamma \gg 1$. Making use of the expansion

$$\left(\frac{1}{2} - s\right) \log \left(\frac{1}{2} - s\right) = \left(\frac{1}{2} - s\right) \log(-s) + \frac{1}{2} + \mathcal{O}\left(\frac{1}{s}\right),$$

we can write the mid-range solution with terms ordered by size as

$$v(s) = \gamma^2 \left(\frac{1}{2} - s\right) + \left(\frac{1}{2} - s\right) \log(-s) + (c-2)s \log \gamma + \left(d + \frac{1}{2}\right)s + a \log \gamma + b + \frac{1}{2}(1 + \log 2) + \mathcal{O}\left(\frac{1}{s}, \frac{1}{\gamma^2}\right). \quad (31)$$

Next, rewrite the inner solution (17) using $v = \gamma^4 u(r)$ and replace

$$r = 1 + \frac{s}{\gamma^2}.$$

Then, assuming that $\gamma^2 \gg -s \gg 1$, we obtain the inner expansion in terms of the mid-range variable:

$$\gamma^4 u \left(1 + \frac{s}{\gamma^2}\right) = \gamma^2 \left(\frac{1}{2} - s\right) - s \log(-s) + 2s \log \gamma + \frac{17}{12} + \frac{1}{2} \log(-s) - \log \gamma + \mathcal{O}\left(\frac{1}{\gamma^2}\right).$$

By comparing this expression with that for the mid-range in (31), we find that all terms match provided the constants satisfy

$$a = -1, \quad b = \frac{11}{12} - \frac{1}{2} \log 2, \quad c = 4, \quad d = -\frac{1}{2}.$$

Therefore, the mid-range solution for $s < 1/2$ is

$$v(s) = \gamma^2 \left(\frac{1}{2} - s\right) + (2s - 1) \log \gamma + \frac{11}{12} + \left(\frac{1}{2} - s\right) \log \left(\frac{1}{2} - s\right) + \mathcal{O}\left(\frac{1}{\gamma^2}\right). \quad (32)$$

Substituting the constants into (27), we also find that to leading order

$$v(0) = \frac{\gamma^2}{2} - \log \gamma + b \quad \text{or} \quad \Theta\left(\frac{1}{\gamma}\right) = \frac{1}{2\gamma^2} + \frac{b - \log \gamma}{\gamma^4}. \quad (33)$$

Similarly, (28) implies that

$$\log v_\infty = -\gamma^2 + 4 \log \gamma - \frac{1}{2} + \mathcal{O}\left(\frac{1}{\gamma^2}\right),$$

so that

$$v_\infty \approx \gamma^4 e^{-\gamma^2 - 1/2} \quad \text{giving} \quad \bar{\beta} = -\log(\Theta_\infty) = \gamma^2 + \frac{1}{2} + \mathcal{O}\left(\frac{1}{\gamma^2}\right). \quad (34)$$

4.3.2. *Mid-range Solution for $s > 1/2$.* To leading order, the right mid-range solution satisfies

$$v' = -\log\left(\frac{v}{v_\infty}\right), \quad (35)$$

which can be integrated when $s > 0$ to obtain

$$s = v_\infty \left[\text{li}\left(\frac{v(0)}{v_\infty}\right) - \text{li}\left(\frac{v}{v_\infty}\right) \right], \quad (36)$$

where

$$\text{li}(z) = \int_0^z \frac{dt}{\log t}$$

is the *logarithmic integral function*. In order to develop the mid-range solution for large s for matching with the outer solution, we must consider the case where $s \rightarrow \infty$ and $v(s)/v_\infty \rightarrow 1$. From (33)–(34), we have that $v(0) \approx \gamma^2/2$ and $v_\infty \approx \gamma^4 \exp(-\gamma^2 - 1/2)$, so that $v(0)/v_\infty \gg 1$ for large γ . This requires estimates of the logarithmic integral $\text{li}(z)$ in the two limits $z \rightarrow 1$ and $z \rightarrow \infty$, which are well-known to be

$$\text{li}(z) = \Gamma_e + \log \log z + \mathcal{O}(\log z) \quad \text{as } z \rightarrow 1, \quad (37)$$

$$\text{li}(z) = \frac{z}{\log z} + \mathcal{O}\left(\frac{z}{\log^2 z}\right) \quad \text{as } z \rightarrow \infty, \quad (38)$$

where $\Gamma_e = 0.57721\dots$ is Euler's constant. Using the expansion (38) for large z , we obtain that

$$\begin{aligned} v_\infty \text{li}\left(\frac{v(0)}{v_\infty}\right) &= \frac{v(0)}{\log(v(0)) - \log(v_\infty)} + \mathcal{O}\left(\frac{v(0)}{\log^2(v_\infty)}\right) \\ &= \frac{\gamma^2/2}{\gamma^2 + \frac{1}{2} - \log 2 - 2\log \gamma} + \mathcal{O}\left(\frac{1}{\gamma^2}\right) \\ &= \frac{1}{2} + \mathcal{O}\left(\frac{1}{\gamma^2}\right). \end{aligned} \quad (39)$$

If we denote $s_* = v_\infty \text{li}(v(0)/v_\infty)$ then Eq. (36) can be written as

$$v_\infty \text{li}\left(\frac{v(s)}{v_\infty}\right) = s_* - s, \quad (40)$$

which can be used to match to the mid-range expression (32). To perform this matching, we consider Eq. (40) when v/v_∞ is large, in which case

$$\begin{aligned} s_* - s = v_\infty \text{li}\left(\frac{v}{v_\infty}\right) &= \frac{v}{\log(v/v_\infty)} + \frac{v}{\log^2(v/v_\infty)} + \mathcal{O}\left(\frac{v}{\gamma^6}\right) \\ &= \frac{v}{\gamma^2 + \frac{1}{2} - 4\log \gamma + \log v} + \frac{v}{\gamma^4} + \mathcal{O}\left(\frac{v}{\gamma^6}\right). \end{aligned} \quad (41)$$

To leading order, this implies that $v/\gamma^2 \approx s_* - s$ or

$$v \approx \gamma^2(s_* - s),$$

which can be reused in the denominator of (40) to obtain the refined approximation

$$\begin{aligned} s_* - s &= \frac{v}{\gamma^2 + \frac{1}{2} - 2 \log \gamma + \log(s_* - s)} + \frac{v}{\gamma^4} + \mathcal{O}\left(\frac{v}{\gamma^6}\right) \\ &= \frac{v}{\gamma^2 - \frac{1}{2} - 2 \log \gamma + \log(s_* - s) + \mathcal{O}(\gamma^{-2})}, \end{aligned}$$

or

$$v = (s_* - s) \left(\gamma^2 - \frac{1}{2} - 2 \log \gamma + \log(s_* - s) + \mathcal{O}\left(\frac{1}{\gamma^2}\right) \right). \quad (42)$$

Because Eq. (35) is only the leading order equation for v , this last result is not sufficient to perform the mid-range matching completely. Consequently, we must return to the next order equation (25)

$$v' = \log v_\infty - \log v + \frac{sv'}{\gamma^2} + \frac{1}{\gamma^2}(v_\infty - v) + \mathcal{O}\left(\frac{1}{\gamma^4}\right). \quad (43)$$

Now, consider v to be a perturbation of the leading order terms of (42), which we denote by \hat{v} and set

$$v = \hat{v} + \varphi, \quad \text{where } \varphi/v \text{ is assumed to be small.}$$

Substituting this expression for v into Eq. (43), we obtain the leading order equation for φ

$$\varphi' = \frac{\varphi}{\gamma^2(s_* - s)} - s_* + \frac{v_\infty}{\gamma^2}. \quad (44)$$

Observe that there is a potential singularity in this expression at $s = s_*$, which then forces the condition $\varphi(s_*) = 0$. Hence, the asymptotically consistent solution is given by

$$\varphi(s) = s_*(s_* - s) + \mathcal{O}\left(\frac{1}{\gamma^2}\right) = \frac{1}{4} - \frac{s}{2} + \mathcal{O}\left(\frac{1}{\gamma^2}\right). \quad (45)$$

Substituting this expression into $v = \hat{v} + \varphi$ along with the right mid-range solution (42) yields

$$v(s) = \gamma^2(s_* - s) - \frac{s_*}{2} - 2(s_* - s) \log \gamma + (s_* - s) \log(s_* - s) + \frac{1}{4} + \mathcal{O}\left(\frac{1}{\gamma^2}\right). \quad (46)$$

This expression can now be matched with the left mid-range solution (32) obtained earlier by introducing a higher order correction

$$s_* = \frac{1}{2} + \frac{A}{\gamma^2},$$

for some constant A to be determined. Substituting this last expression into (46) yields

$$\hat{v} = \gamma^2 \left(\frac{1}{2} - s \right) + A - \frac{1}{4} - 2 \left(\frac{1}{2} - s \right) \log \gamma + \left(\frac{1}{2} - s \right) \log \left(\frac{1}{2} - s \right) + \frac{1}{4}, \quad (47)$$

and all terms in (47) and (32) match provided that $A = \frac{11}{12}$. Hence, we deduce that to this order

$$s_* = \frac{1}{2} + \frac{11}{12\gamma^2}, \quad (48)$$

and the leading order equation for the mid-range solution is given implicitly by

$$s = \frac{1}{2} + \frac{11}{12\gamma^2} - v_\infty \operatorname{li} \left(\frac{v(s)}{v_\infty} \right). \quad (49)$$

Now, consider the limit as $s \rightarrow \infty$ for which the mid-range solution takes the form $v(s)/v_\infty = 1 + h(s)$ for $0 < h \ll 1$. It follows from (37) that

$$\begin{aligned} \operatorname{li}(v(s)/v_\infty) &= \operatorname{li}(1 + h) = \Gamma_e + \log h + \mathcal{O}(h), \\ &\approx \Gamma_e + \log(v(s)/v_\infty - 1). \end{aligned}$$

This leads to the following elegant expression for the mid-range solution at large values of $s > 0$

$$v(s) = v_\infty \left[1 + \exp \left(-\Gamma_e - \frac{s - s_*}{v_\infty} \right) \right] \quad \text{where} \quad s_* = \frac{1}{2} + \frac{11}{12\gamma^2}, \quad (50)$$

as well as its derivative

$$v'(s) = -\exp \left(-\Gamma_e - \frac{s - s_*}{v_\infty} \right). \quad (51)$$

These expressions clearly demonstrate the existence of a sharp corner in the solution at the point $s = s_*$.

4.4. Wetting Front Location

The point s_* is a good candidate for the location of the wetting front and corresponds to

$$y_* = \frac{1}{\gamma} + \frac{1}{2\gamma^3} + \frac{11}{12\gamma^5} + \mathcal{O} \left(\frac{1}{\gamma^7} \right) \quad (52)$$

in the original variables, which is consistent with the approximation (20) found earlier in the derivation of the inner solution. This formula for y_* is now derived more carefully. Recall that we defined the wetting front location y_{**} as the point where the curvature Θ'' takes on a maximum value, so that $\Theta'''(y_{**}) = 0$. Differentiating the original ODE (8a) yields

$$\Theta\Theta''' + \Theta'\Theta'' = -y\Theta'' - \Theta',$$

so that imposing $\Theta'''(y_{**}) = 0$ yields at $y = y_{**}$

$$\Theta' = -\frac{y\Theta''}{1 + \Theta''}.$$

Assuming that that $y_{**} \approx 1/\gamma$ and $\Theta''(y_{**}) \gg 1$ (both to be justified shortly), we have to leading order that

$$\Theta'(y_{**}) = -\frac{1}{\gamma}.$$

However, based on the mid-range equation derived earlier, we also have

$$\Theta' = -\frac{1}{\gamma} \log \left(\frac{\Theta}{\Theta_\infty} \right),$$

and so it follows immediately that the maximum value of Θ'' arises when

$$\log \left(\frac{\Theta}{\Theta_\infty} \right) = 1 \quad \text{or} \quad \Theta(y_{**}) = e\Theta_\infty. \quad (53)$$

Substituting these approximations for y_{**} , $\Theta(y_{**})$ and $\Theta'(y_{**})$ into the ODE $\Theta'' = -y\Theta'/\Theta$, we find that to leading order the maximum value of Θ'' at $y = y_{**}$ is given by

$$\max \Theta'' \approx \frac{1}{\gamma^2 e \Theta_\infty} = \frac{e^{\gamma^2 - 1/2}}{\gamma^2}, \quad (54)$$

where we have also used Eq. (34). As expected, this is indeed very large for even moderately large value γ (which incidentally leads to severe problems in any numerical scheme that attempts to compute for large γ).

The wetting front location may now be estimated by substituting (53) into (36). In this expression the front occurs when $v(s)/v_\infty = e$, which is given by

$$s_{**} = v_\infty \left[\text{li} \left(\frac{v(0)}{v_\infty} \right) - \text{li}(e) \right],$$

and our previous asymptotic analysis yields

$$s_{**} = \frac{1}{2} + \frac{11}{12\gamma^2} + \mathcal{O} \left(\frac{1}{\gamma^4} \right) - v_\infty \text{li}(e).$$

Ignoring exponentially small terms and rescaling, we then obtain

$$y_{**} = \frac{1}{\gamma} + \frac{1}{2\gamma^3} + \frac{11}{12\gamma^5} + \mathcal{O} \left(\frac{1}{\gamma^7} \right), \quad (55)$$

which to this order of asymptotics is identical to the expression for y_* in (52) that was identified with the corner s_* in the derivation of the mid-range solution.

4.5. Outer Solution, and Matching to Mid-range Solution

Within the outer region we have that $\Theta \rightarrow \Theta_\infty$ as $y \rightarrow \infty$. So we will take the outer region to consist of those y values for which Θ is close to Θ_∞ and look for a solution that is a small perturbation from a constant, namely

$$\Theta(y) = \Theta_\infty(1 + g(y)), \quad (56)$$

where both $|g|$, $|g'| \ll 1$ for y sufficiently large. After substituting this expression into (8a), we obtain

$$g' = -\frac{\Theta_\infty}{y} (1 + g) g'',$$

which can be approximated for small $|g|$ by

$$\Theta_\infty g'' = -y g'$$

This equation can be integrated once to obtain

$$g' = -A \exp \left(-\frac{y^2}{2\Theta_\infty} \right), \quad (57)$$

where $A > 0$ is a constant that is independent of Θ_∞ (noting that A must be positive in order that both g' and Θ' are negative and hence have the required decreasing behaviour at infinity). A second integration yields

$$g(y) = A \sqrt{\frac{\pi\Theta_\infty}{2}} \text{erfc} \left(\frac{y}{\sqrt{2\Theta_\infty}} \right), \quad (58)$$

where $\operatorname{erfc}(z) = \int_z^\infty e^{-\zeta^2} d\zeta$ is the *complementary error function*. We now aim to find the constant A by matching g' with the derivative of the mid-range solution by letting $y = 1/\gamma + s/\gamma^3$ with s/γ^2 small and $v_\infty = \gamma^4 \theta_\infty$. Substituting into the outer solution derivative (57) yields

$$\frac{dg}{dy} = -A \exp\left(-\frac{1}{2\gamma^2\Theta_\infty} - \frac{s}{v_\infty}\right).$$

We may then replace the outer variable g using the scaling

$$\frac{dv}{ds} = \frac{v_\infty}{\gamma^3} \frac{dg}{dy},$$

so that the derivative of the outer solution written in terms of the mid-range variables is

$$\frac{dv}{ds} = -\frac{v_\infty A}{\gamma^3} \exp\left(-\frac{1}{2\gamma^2\Theta_\infty} - \frac{s}{v_\infty}\right) = -\frac{v_\infty A}{\gamma^3} \exp\left(-\frac{\gamma^2}{2v_\infty} - \frac{s}{v_\infty}\right).$$

We then need to compare this expression with the mid-range solution derivative, which from (51) is

$$v'(s) = -\exp\left(-\Gamma_e + \frac{1}{2v_\infty} - \frac{s}{v_\infty}\right).$$

These last two equations match exactly provided that

$$A = \frac{\gamma^3}{v_\infty} \exp\left(-\Gamma_e + \frac{(1 + \gamma^2)}{2v_\infty}\right), \quad (59)$$

and taken together with Eqs. (56) and (58) this completes the outer solution.

4.6. Asymptotic Expansion for γ

We have so far expressed all asymptotic expansions in terms of the large parameter γ . However, γ is not actually known *a priori* for a physical problem and so instead it is preferable to write γ in terms of the known parameter $\bar{\beta}$. Taking the result from (34), we have that

$$\bar{\beta} = \gamma^2 + \frac{1}{2} + \frac{\alpha_3}{\gamma^2} + \mathcal{O}\left(\frac{1}{\gamma^4}\right), \quad (60)$$

where we have introduced the coefficient α_3 that is yet to be determined. Neglecting the $\mathcal{O}(\gamma^{-4})$ terms yields a quadratic equation for γ^2 whose solution can be expressed for large $\bar{\beta}$ as

$$\gamma = \bar{\beta}^{1/2} - \frac{1}{4}\bar{\beta}^{-1/2} - \left(\frac{\alpha_3}{2} + \frac{1}{32}\right)\bar{\beta}^{-3/2} + \mathcal{O}\left(\bar{\beta}^{-5/2}\right). \quad (61)$$

The high fidelity numerical calculations reported by Amodio et al. [1] provide convincing numerical evidence that

$$\alpha_3 = \frac{1}{12},$$

although we have no formal calculation as yet to confirm this result.

4.7. Summary of Composite Asymptotic Solution

Here we present a concise summary of the leading order asymptotic approximations for the inner, mid-range and outer solutions derived in Eqs. (17), (32), (50), (56), (58) and (59), expressing each

in terms of the similarity variable $\Theta(y)$ as follows:

$$\begin{array}{l} \text{Inner:} \\ (0 \leq y < \gamma^{-1}) \end{array} \quad \Theta(y) \approx 1 - \gamma y + \frac{1}{\gamma^2} \left[\frac{1}{2} - \frac{1}{2}(1 - \gamma y)^2 + (1 - \gamma y) \log(1 - \gamma y) \right], \quad (62a)$$

$$\begin{array}{l} \text{Left mid-range:} \\ (\gamma^{-1} < y < y_*) \end{array} \quad \Theta(y) \approx \frac{1}{\gamma}(y_* - y) [\gamma^2 + \log \gamma + \log(y_* - y)], \quad (62b)$$

$$\begin{array}{l} \text{Right mid-range:} \\ (y > y_*) \end{array} \quad \Theta(y) \approx \Theta_\infty + \Theta_\infty \exp\left(-\Gamma_e - \frac{y - y_*}{\gamma \Theta_\infty}\right), \quad (62c)$$

$$\begin{array}{l} \text{Outer:} \\ (y \rightarrow \infty) \end{array} \quad \Theta(y) \approx \Theta_\infty + \frac{1}{\gamma} \sqrt{\frac{\pi \Theta_\infty}{2}} \exp\left(-\Gamma_e + \frac{1 + \gamma^2}{2\gamma^4 \Theta_\infty}\right) \operatorname{erfc}\left(\frac{y}{\sqrt{2\Theta_\infty}}\right). \quad (62d)$$

In these above expressions, $\Theta_\infty = e^{-\bar{\beta}}$ and γ can be written in terms of $\bar{\beta}$ as

$$\gamma \approx \bar{\beta}^{1/2} - \frac{1}{4} \bar{\beta}^{-1/2} - \left(\frac{\alpha_3}{2} + \frac{1}{32}\right) \bar{\beta}^{-3/2}. \quad (62e)$$

This last equation may also be used to replace γ in the expansion of the front location from (52) to yield

$$y_* \approx \bar{\beta}^{-1/2} + \frac{3}{4} \bar{\beta}^{-3/2} + \left(\frac{\alpha_3}{2} + \frac{133}{96}\right) \bar{\beta}^{-5/2}, \quad (62f)$$

where $\alpha_3 = \frac{1}{12}$ (numerically).

5. Other Asymptotic Approximations

In this section, we present two alternative asymptotic solutions to the exponential diffusion problem that are derived using other methods.

5.1. Babu's Solution

Babu [2] studied a modified version of the exponential diffusion problem in which he made the approximating assumption that that beyond some finite distance $y \geq y_*$ the saturation is identically equal to the residual value. In other words, he solves a modified ODE boundary value problem that replaces our Eqs. (8) with the following:

$$\Theta \Theta'' = -y \Theta' \quad \text{for } 0 < y < y_*, \quad (63a)$$

$$\Theta(0) = 1, \quad (63b)$$

$$\Theta(y_*) = \Theta_\infty, \quad (63c)$$

$$\frac{d\Theta}{dy} \rightarrow 0 \quad \text{as } y \rightarrow y_*. \quad (63d)$$

Here, the front location y_* is an unknown constant that must be determined as part of the solution and consequently an extra right-hand boundary condition (63d) has had to be imposed (which corresponds physically to requiring a zero water flux at y_*). By expanding the solution as a series

in $\eta = (1 - \Theta_\infty)/\bar{\beta}$, Babu obtained the following approximation for the wetting front location

$$y_*^B = \eta^{1/2} \left[1 + \frac{1}{3}\eta + \left(\frac{17}{90} + \frac{\bar{\beta}}{8} \right) \eta^2 + \dots \right], \quad (64a)$$

where we have used a superscript ‘‘B’’ to distinguish Babu’s solution. If we neglect exponentially small terms involving $\Theta_\infty = e^{-\bar{\beta}}$, then this expression can be rewritten in terms of $\bar{\beta}$ as

$$y_*^B \approx \bar{\beta}^{-1/2} + \frac{11}{24}\bar{\beta}^{-3/2} + \mathcal{O}\left(\bar{\beta}^{-5/2}\right), \quad (64b)$$

which may then be compared directly to our asymptotic approximation in (62f). Although the leading order term in each series of $\mathcal{O}\left(\bar{\beta}^{-1/2}\right)$ is identical, the discrepancy between coefficients in the next order terms generates a significant difference in the front locations. Babu also derived two further approximations that he refers to as a second order expansion

$$\Theta^{B,2}(y) = 1 + \bar{\beta}\eta^{1/2} \left(\frac{\eta}{6}y - y + \frac{1}{6}y^3 \right), \quad (64c)$$

and third order expansion

$$\Theta^{B,3}(y) = \Theta^{B,2}(y) + \bar{\beta}\eta^{1/2} \left[\left(\frac{7}{360} + \frac{\bar{\beta}}{24} \right) \eta^2 y - \frac{\eta}{36}y^3 + \frac{\bar{\beta}\eta^{1/2}}{12}y^4 - \frac{1}{40}y^5 \right], \quad (64d)$$

both of which are defined on the interval $0 \leq y \leq y_*^B$. When $y > y_*^B$, the saturation in both cases satisfies $\Theta^{B,2} = \Theta^{B,3} = \Theta_\infty$ (corresponding to $\bar{\theta} = 0$). Babu’s solution is simpler than the one derived in this paper in that it is a polynomial expansion in integer powers of y and requires no multi-layer matching. However, this simplicity comes at the expense of reduced accuracy as well as a lack of information about the detailed structure of the wetting front. One particular disadvantage of Babu’s approach is that none of the approximations for Θ is continuous at $y = y_*^B$.

5.2. Parlange’s Solution

Parlange [12, 13] developed an iterative approach for solving the nonlinear diffusion equation based on the *Bruce-Klute equation*

$$D(\theta) = -\frac{dy}{d\theta} \int_{\theta_0}^{\theta} y(\alpha) d\alpha, \quad (65)$$

which can be derived by treating y as a function of saturation θ . Parlange then applied a number of simplifications to obtain an approximate formula for y in terms of integrals of the diffusivity. For the specific case of an exponential diffusivity, Parlange [13] derived an implicit asymptotic representation for the saturation which can be expressed in terms of our similarity variables as

$$y = \left(\bar{\beta}^{-1/2} + \bar{\beta}^{-3/2} \right) \left(1 - \Theta^P + \Theta^P \log \Theta^P / \bar{\beta} \right). \quad (66a)$$

In a similar manner to Babu’s solution, Parlange also imposed the condition that $\Theta \equiv \Theta_\infty = e^{-\bar{\beta}}$ for all $y \geq y_*^P$. Equating terms in Eq. (66a) gives the result

$$y_*^P = \left(\bar{\beta}^{-1/2} + \bar{\beta}^{-3/2} \right) \left(1 - 2e^{-\bar{\beta}} \right). \quad (66b)$$

Intriguingly, this estimate involves an exponential term that would correspond to a ‘‘beyond all orders’’ contribution to the results in this paper. This estimate behaves asymptotically in the limit

of large $\bar{\beta}$ as

$$y_*^P \approx \bar{\beta}^{-1/2} + \bar{\beta}^{-3/2}, \quad (67)$$

from which it is clear that the front location matches only at leading order with our estimate (62f) and that of Babu from (64b).

Another related solution has been derived from the Bruce-Klute equation by Parlange et al. [14], who extended an earlier method of Heaslet and Alksne [9] for the power-law diffusivity to the exponential case. This solution also has a representation as an implicit equation in Θ , but this time involves the exponential integral function, $\text{Ei}(z)$. Because evaluating Θ requires inverting Ei , their solution is much more complicated and expensive to compute than ours and so we have not considered it here.

6. Comparison of Asymptotic and Numerical Results

We now compare the various asymptotic solutions presented in the preceding sections. We also validate the asymptotic results using numerical simulations of the initial value problem in Eqs. (8') based on an algorithm that is described next.

6.1. Solution Algorithm

The ODE (8a) for the similarity variable $\Theta(y)$ is integrated over an interval $y \in [0, L]$ using the MATLAB initial value solver `ode15s`. Since both the problem and our asymptotic results correspond to $L = \infty$, we must choose L sufficiently large that any error arising from truncating the right-hand boundary does not pollute the solution in the interior; on the other hand, $\Theta(y)$ tends quite rapidly toward Θ_∞ as y increases beyond the front, and so L does not need not be taken much larger than y_* . In practice, we have find that choosing $L = 2\bar{\beta}^{-1/2}$ (twice the leading order estimate of the wetting front location) provides a reasonable compromise between efficiency and accuracy.

For an actual wetting scenario, we know the asymptotic saturation Θ_∞ (from $\bar{\beta}$), but the value of γ in the second initial condition is not known *a priori*. We therefore build the initial value solver into a shooting type algorithm, for which we guess the slope $\gamma = -\Theta'(0)$, integrate the saturation variable to $\Theta(L)$, and then compare to the target value Θ_∞ . The slope γ is then modified using a binary search procedure and this integration procedure is iterated until the relative error in the right boundary condition satisfies $|\Theta(L) - \Theta_\infty|/\Theta_\infty < \text{TOL}$, where TOL is a given tolerance. The leading term $\gamma \approx \bar{\beta}^{1/2}$ from the asymptotic formula (62e) provides a sufficiently accurate initial guess to begin the iteration, and choosing ODE tolerances of $\text{ABSTOL} = \text{RELTOL} = 10^{-10}$ and Θ -tolerance of $\text{TOL} = 10^{-6}$ yields a computed solution that for all intents and purposes can be treated as an “exact solution” of the original problem.

A significant difficulty with this algorithmic approach is that for even moderate values of γ the solution curvature near the wetting front is on the order of $\exp(\gamma^2)$, which can be extremely large. This large curvature causes problems with the initial value solver we are using, and effectively limits the maximum value of $\bar{\beta}$ to roughly 20, which restricts $\gamma \lesssim 4.4$. With this restricted range of γ , we can still test the validity of the asymptotic formulae derived here but we are not able to see their true accuracy at larger γ , as the asymptotic series we have derived only converge at a polynomial rate as γ increases. Consequently, we will also report some results using a much more sophisticated numerical approach that is the subject of a related paper [1] and which employs a high-order Taylor expansion based boundary value solver coupled with mesh adaptivity. This method permits calculations up to $\gamma = 18$, corresponding to $\bar{\beta} \approx 325$ and $\theta_\infty \approx 1.18 \times 10^{-141}$.

6.2. Saturation Profiles

Plots of the multi-layer asymptotic solution determined by Eqs. (62) are depicted in Figure 7 for values of $\bar{\beta} = 4, 8$ and 16 alongside the corresponding plots of the computed solution using the shooting method described above (which can essentially be considered as an “exact solution”). The inner and mid-range solution are both displayed, and the loss of asymptotic validity of the inner solution due to the logarithmic term is evident as $y \rightarrow y_*$. We have included in all plots the corresponding asymptotic solutions of Babu [2] and Parlange [13], and in each case a second plot of all curves in terms of the rescaled saturation θ is given (lower plots), which accentuates differences in the wetting front location. Our asymptotic solution is clearly an improvement over Babu’s solution for all values of $\bar{\beta}$, which we attribute in large part to the fact that Babu’s approximation truncates the saturation at some approximate wetting front location and ignores the details of the solution structure within and to the right of the front.

As described above, the relatively slow convergence of our asymptotic solution, which is polynomial in γ , and hence also in $\bar{\beta}$, means that our asymptotic approximation is not particularly accurate for smaller values of $\bar{\beta}$ such as $\bar{\beta} = 4$. This is reflected in the mismatch between the left and right mid-range solution at the wetting front location (represented by the blue triangular point). However, our asymptotic approximation improves significantly in accuracy as $\bar{\beta}$ increases, and when we take $\bar{\beta} = 16$ the comparison between the computed and asymptotic results are good. The differences at even larger $\bar{\beta}$ are difficult to visualize using saturation plots, and so we compare the solutions further in the next sections in terms of the estimates for wetting front location.

6.3. Wetting Front Location y_*

We next focus on calculations of the wetting front location y_* , which we have defined in our derivation to be the point where Θ' is a maximum. A visual comparison is provided in Figure 8 in terms of the computed front location as a function of $\bar{\beta}$, showing our asymptotic estimate y_*^{asy} from (62f), Babu’s estimate y_*^B given in (64d), and Parlange’s estimate y_*^P given in (67). We also included numerical estimates of front location using the Matlab solver `ode15s`, for which we were able to compute up to a maximum of $\bar{\beta} \approx 20$ before the ODE solver failed. The plot of error in front location (relative to the computed solution) clearly shows that although Parlange’s estimate is better than our asymptotic solution for some values of $\bar{\beta} \gtrsim 10$, our result is consistently superior for larger $\bar{\beta}$; indeed, even our two-term asymptotic solution surpasses Parlange’s result when $\bar{\beta} \gtrsim 13$.

Although our simple numerical approach fails for $\bar{\beta} > 20$, a more sophisticated numerical algorithm has been implemented by Amodio et al. [1] that yields accurate solutions for values of $\bar{\beta}$ much larger. Their results for a much wider range of $\bar{\beta}$ are summarized in Table 1, along with the corresponding asymptotic results for y_*^{asy} , y_*^B and y_*^P . The superior accuracy of our asymptotic solution for large $\bar{\beta}$ when compared with Babu’s and Parlange’s approximations is evident upon comparing the computed value of y_* to the three asymptotic approximations.

Table 1

Comparison of our asymptotic results to computations using the method of Amodio et al. [1].

γ	Computed results			Asymptotic results		
	$\bar{\beta}$	θ_∞	y_*	y_*^{asy}	y_*^B	y_*^P
2	4.559435	1.046797e-2	0.571747	0.54536	0.51539	0.57103
6	36.50238	1.403505e-16	0.16911	0.1689165	0.16759	0.170050
10	100.5008	2.254440e-44	0.1005094	0.1004949	0.100205	0.100743
18	324.5002	1.178490e-141	0.0556417	0.0556410	0.0055591	0.055683

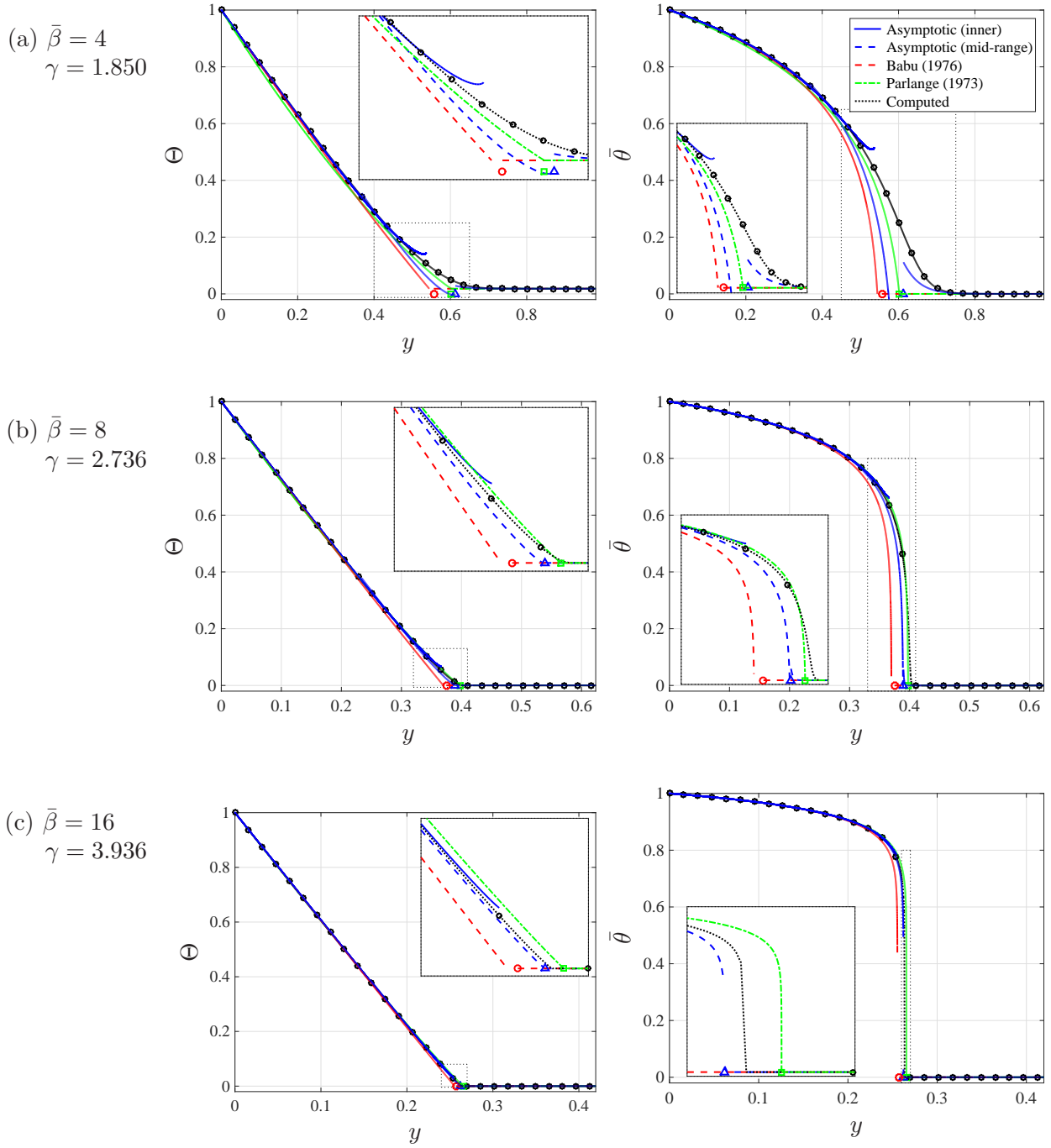


Figure 7. Comparison of our asymptotic solution (—) to those of Babu (---) and Parlange (····) for $\bar{\beta} = 4, 8$ and 16 , displayed in terms of the similarity variable (left) and rescaled saturation (right). The corresponding approximations of the wetting front location are denoted by points lying on the y -axis for our asymptotics (\triangle), Babu (\circ) and Parlange (\square).

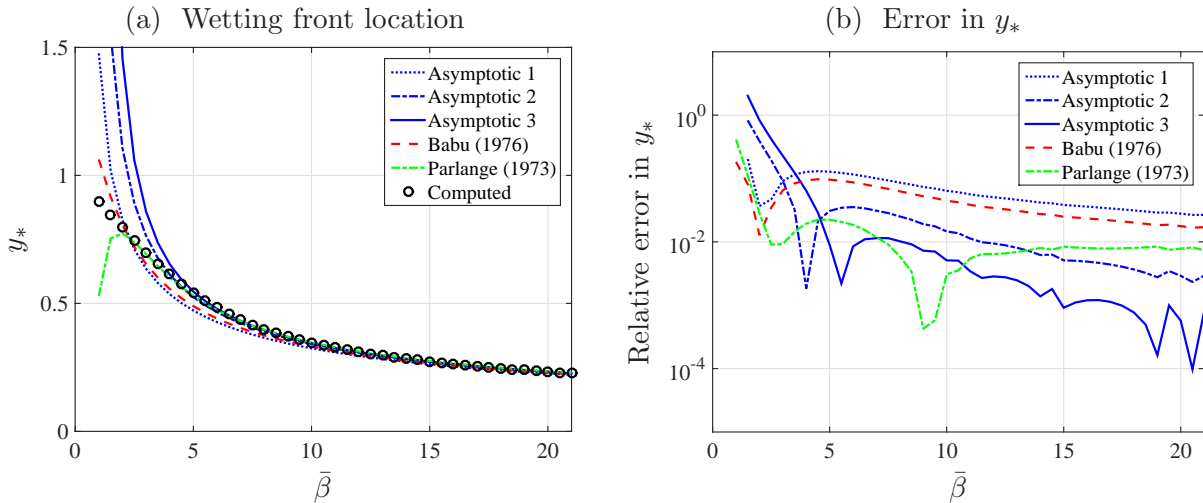


Figure 8. Comparison of the various asymptotic estimates for wetting front location y_* to the computed (“exact”) solution.

6.4. Initial Slope γ

Finally, we investigate the accuracy of our asymptotic approximation for γ in Eq. (62e), for which no corresponding estimate is available from Babu or Parlange. For a range of $\bar{\beta}$, Figure 9 compares the value of γ determined from shooting simulations with that obtained from the 1-, 2- and 3-term asymptotic estimates. The accuracy of our series approximation is evident for increasing values of $\bar{\beta}$, which is essential because γ is a required input for our numerical simulations and yet it is the parameter $\bar{\beta}$ and not γ that is known *a priori* for any given physical wetting scenario.

We finish by restating some of the numerical results obtained in [1] for values of γ as high as 18 (corresponding to β up to 324). Beyond this range, even this more sensitive algorithm was unable to converge owing to the size of θ'' at the wetting front. The primary calculations of y_* and θ_∞ over a range of values of γ were then enhanced by using Richardson extrapolation. The primary contribution of [1] was to provide clear numerical evidence to support the validity of the following expressions

$$y_* \approx \frac{1}{\gamma} + \frac{1}{2\gamma^3} + \frac{11}{12\gamma^5} + \frac{2.96}{\gamma^7},$$

and

$$\bar{\beta} = -\log(\theta_\infty) \approx \gamma^2 + \frac{1}{2} + \frac{1}{12\gamma^2} + \frac{0.089}{\gamma^4},$$

which extends the asymptotics derived in this paper by one additional term. These results are in full agreement with our asymptotics and also hint at a more refined asymptotic calculation.

7. Conclusions

In this paper we have performed a multi-layer asymptotic analysis of a problem in wetting front formation governed by the nonlinear diffusion equation, for which the diffusion coefficient is an exponential function of saturation, $D(\theta) = D_o e^{\beta\theta}$. Motivated by the structure of the wetting front

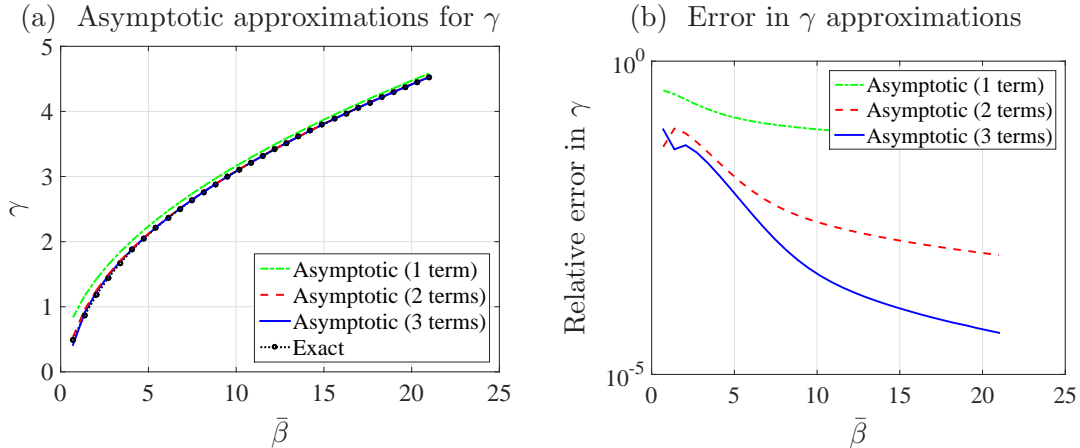


Figure 9. Comparison of the various asymptotic approximations of γ based on retaining one, two or three terms from the series in Eq. (62e). The left hand plot compares the three asymptotic results to the value of γ obtained using the shooting algorithm. The right hand plot depicts the corresponding absolute error in the asymptotic approximations, treating the shooting results as the “exact” solution.

for large values of β , we used the method of matched asymptotics to derive a four-layer solution consisting of a different asymptotic series for each of four regions corresponding to the wetting, and the leading and trailing edges. Other previous approaches to deriving (approximate) analytical solutions have assumed that the reduced saturation is identically equal to zero at a finite wetting front location, which essentially ignores the structure of the *sharp corner* that appears at the front for large β . In contrast, our asymptotic solution uncovers the detailed structure of the transition within the wetting front, where the solution has very high curvature, and is considerably more accurate than other previous approaches for large values of β . The asymptotic solution converges polynomially in β and maintains a high degree of accuracy over a wide range of β values corresponding to physical porous media such as soils and rock, unlike many other approaches which are either more limited in their applicability or exhibit a logarithmic singularity near the wetting front as β becomes large. Our approach has the additional advantage that it expresses the solution in terms of explicit formulas instead of requiring numerical approximation of a differential equation (which is required in the approaches of Wagner [22] or Shampine [19]) or inverting the exponential integral function (as in Parlange et al.’s asymptotic solution [14]).

Acknowledgments

This work was funded by grants from the Natural Sciences and Engineering Research Council of Canada, Mitacs Network of Centres of Excellence, Pacific Institute for the Mathematical Sciences, and Engineering and Physical Sciences Research Council.

References

1. P. AMODIO, C. J. BUDD, O. KOCH, G. SETTANNI, AND E. B. WEINMÜLLER, *Asymptotical computations for a*

- model of flow in saturated porous media*, Appl. Math. Comput., 237 (2014), pp. 155–167.
2. D. K. BABU, *Infiltration analysis and perturbation methods. 1. Absorption with exponential diffusivity*, Water Resour. Res., 12 (1976), pp. 89–93.
 3. J. BEAR, *Dynamics of Fluids in Porous Media*, Dover, New York, 1988.
 4. W. BRUTSAERT, *Universal constants for scaling the exponential soil water diffusivity?*, Water Resour. Res., 15 (1979), pp. 481–483.
 5. B. E. CLOTHIER AND I. WHITE, *Measurement of sorptivity and soil water diffusivity in the field*, Soil Sci. Soc. Amer. J., 45 (1981), pp. 241–245.
 6. L. Y. COOPER, *Constant temperature at the surface of an initially uniform temperature, variable conductivity half space*, J. Heat Transfer, 93 (1971), pp. 55–60.
 7. J. CRANK, *The Mathematics of Diffusion*, Oxford University Press, second ed., 1975.
 8. C. M. ELLIOTT, M. A. HERRERO, J. R. KING, AND J. R. OCKENDON, *The mesa problem: Diffusion patterns for $u_t = \nabla \cdot (u^m \nabla u)$ as $m \rightarrow +\infty$* , IMA J. Appl. Math., 37 (1986), pp. 147–154.
 9. M. A. HEASLET AND A. ALKSNE, *Diffusion from a fixed surface with a concentration-dependent coefficient*, J. Soc. Indust. Appl. Math., 9 (1961), pp. 584–596.
 10. C. LEECH, D. LOCKINGTON, AND P. DUX, *Unsaturated diffusivity functions for concrete derived from NMR images*, Matér. Constr., 36 (2003), pp. 413–418.
 11. R. D. MILLER AND E. BRESLER, *A quick method for estimating soil water diffusivity functions*, Soil Sci. Soc. Amer. J., 41 (1977), pp. 1020–1022.
 12. J.-Y. PARLANGE, *Theory of water-movement in soils: 1. One-dimensional absorption*, Soil Sci., 111 (1971), pp. 134–137.
 13. ———, *A note on a three-parameter soil-water diffusivity function – Application to the horizontal infiltration of water*, Soil Sci. Soc. Amer. J., 37 (1973), pp. 318–319.
 14. M. B. PARLANGE, S. N. PRASAD, J.-Y. PARLANGE, AND M. J. M. RÖMKENS, *Extension of the Heaslet-Alksne technique to arbitrary soil water diffusivities*, Water Resour. Res., 28 (1992), pp. 2793–2797.
 15. J. PARSLow, D. LOCKINGTON, AND J.-Y. PARLANGE, *A new perturbation expansion for horizontal infiltration and sorptivity estimates*, Transp. Porous Media, 3 (1988), pp. 133–144.
 16. L. PEL, *Moisture transport in porous building materials*, PhD thesis, Technische Universiteit Eindhoven, Feb. 1995.
 17. K. D. REICHARDT, D. R. NIELSEN, AND J. W. BIGGAR, *Scaling of horizontal infiltration into homogeneous soils*, Soil Sci. Soc. Amer. Proc., 36 (1972), pp. 241–245.
 18. L. F. SHAMPINE, *Concentration-dependent diffusion. II. Singular problems*, Quart. Appl. Math., 31 (1973), pp. 287–293.
 19. ———, *Some singular concentration dependent diffusion problems*, Z. angew. Math. Mech., 53 (1973), pp. 421–422.
 20. W. T. SIMPSON, *Determination and use of moisture diffusion coefficient to characterize drying of northern red oak (Quercus rubra)*, Wood Sci. Tech., 27 (1993), pp. 409–420.
 21. J. L. VÁZQUEZ, *The Porous Medium Equation: Mathematical Theory*, Oxford Mathematical Monographs, Clarendon Press, Oxford, 2007.
 22. C. WAGNER, *Diffusion of lead chloride in solid silver chloride*, J. Chem. Phys., 18 (1950), pp. 1227–1230.
 23. W. W.-G. YEH AND J. B. FRANZINI, *Moisture movement in a horizontal soil column under the influence of an applied pressure*, J. Geophys. Res., 71 (1968), pp. 5151–5157.

DEPARTMENT OF MATHEMATICAL SCIENCES, UNIVERSITY OF BATH, BATH, UNITED KINGDOM, BA2 7AY

DEPARTMENT OF MATHEMATICS, SIMON FRASER UNIVERSITY, BURNABY, BC, CANADA, V5A 1S6